

## Outgrowth of Neurites from N1E-115 Neuroblastoma Cells Is Prevented on Repulsive Substrates through the Action of PAK

Katharine J. M. Marler,<sup>1</sup> Robert Kozma,<sup>1,2,†</sup> Sohail Ahmed,<sup>1,2,‡</sup> Jing-Ming Dong,<sup>1,2</sup> Christine Hall,<sup>1</sup> and Louis Lim<sup>1,2,\*</sup>

*Department of Molecular Neuroscience, Institute of Neurology, University College London, 1 Wakefield St., London WC1N 1PJ, United Kingdom,<sup>1</sup> and GSK-IMCB Group, Institute of Molecular & Cell Biology, Proteos, 61 Biopolis Dr., Singapore 138673, Singapore<sup>2</sup>*

Received 25 August 2004/Returned for modification 21 October 2004/Accepted 17 March 2005

**In the central nervous system (CNS), damaged axons are inhibited from regeneration by glial scars, where secreted chondroitin sulfate proteoglycan (CSPG) and tenascin repulse outgrowth of neurites, the forerunners of axons and dendrites. During differentiation, these molecules are thought to form boundaries for guiding neurons to their correct targets. In neuroblastoma N1E-115 cells, outgrowth of neurites on laminin could be induced by serum starvation or inhibition of RhoA by *Clostridium botulinum* C3 toxin. The outgrowing neurites avoided crossing onto the repulsive substrate CSPG or tenascin. This avoidance response was partially overcome on expression of membrane-targeted and kinase-inactive forms of PAK. In these cells, the endogenous PAK isoforms colocalized with actin in distinctive sites,  $\alpha$ PAK in the cell center as small clusters and along the neurite shaft and  $\beta$ PAK and  $\gamma$ PAK in areas with membrane ruffles and filopodia, respectively. When isoform-specific N-terminal PAK sequences were introduced to interfere with PAK function, substantially more neurites crossed onto CSPG when cells contained a  $\gamma$ PAK-derived peptide but not the corresponding  $\alpha$ PAK- or  $\beta$ PAK-derived peptide. Thus, while neurite outgrowth can be promoted by RhoA inhibition, overcoming the accompanying repulsive guidance response will require modulation of PAK activity. These results have therapeutic implications for CNS repair processes.**

The failure of the adult mammalian central nervous system (CNS) to regenerate after injury may in part be due to the inhibitory nature of the glial scar that forms, preventing the damaged axons from regenerating, leading to loss of function (10, 37). The glial scar is a combination of damaged cells, invading cells, and their associated secreted molecules such as chondroitin sulfate proteoglycan (CSPG) and tenascin, which form both a physical and chemical barrier to extending axons (10, 30, 42). In the developing cerebral cortex, tenascin-C is transiently expressed at the boundaries of migratory pathways (17). In the peripheral nervous system, tenascin-C expression correlates with increased cell migration and axonal growth (5). Members of the CSPG family are the major proteoglycans expressed in the nervous system by both neurons and glia (27). Like tenascin-C, CSPGs are believed to form boundaries to guide neurons to their appropriate targets and prevent them making connections with inappropriate targets (23, 52). In the absence of a glial scar, adult rat dorsal root ganglia (DRG) transplanted into adult rat white matter are able to extend axons from the graft boundary (7). Up-regulation of CSPG at the graft boundary was associated with the failure of the DRG to enter the host white matter (7). These and other observations on

myelin and its derivatives support a role for glial scar components, particularly CSPG, in preventing regeneration in the adult CNS.

For functional recovery, neurons are required to regenerate or repair axons that have to skirt or grow through the glial scar and then reconnect with their appropriate targets. Morphogenesis of the precursor neurites and axons crucially involves the actin cytoskeleton, which is subject to regulation by the Rho family GTPases (19, 20, 35, 38, 39, 47). The activation of Rac1 is required for nerve growth factor-induced neurite outgrowth in PC12 cells and can be blocked through injection of dominant negative Rac1 N17 (6). In N1E-115 cells, both Rac1 and Cdc42 are required for outgrowth (20). This can be achieved through the activation of Rac1 either directly or indirectly via prior activation of Cdc42, which antagonizes the activation of RhoA and prevents neurite collapse (20, 47). The involvement of RhoA in growth cone collapse and neurite retraction has been shown in both primary neurons and cultured cells like N1E-115 and PC12 cells (15, 20, 36, 46). Both RhoA and Rac1 have been shown to be involved in different pathways that lead to growth cone collapse in response to inhibitory cues. In the case of ephrin A5-mediated collapse in retinal ganglion cell (RGC) growth cones, RhoA and its downstream effector ROK are required (50). However, Rac1 has also been shown to mediate the collapse of DRG neurons in response to Sema3A (collapsin-1) (16, 49).

N1E-115 neuroblastoma cells provide a facile model for studying how the Rho GTPases participate in guidance signaling pathways initiated by inhibitory substrates. The use of these cells has provided much information on the role of GTPases and effectors in neurite outgrowth and in retraction processes required for guidance or avoidance (12, 14, 20, 40). Unlike

\* Corresponding author. Mailing address: Department of Molecular Neuroscience, Institute of Neurology, University College London, 1 Wakefield St., London WC1N 1PJ, United Kingdom. Phone: (44) 207 2781552. Fax: (44) 207 2787045. E-mail: l.lim@ion.ucl.ac.uk.

† Present address: Genome Institute of Singapore, 60 Biopolis St., Singapore 138672.

‡ Present address: Institute of Molecular & Cell Biology, 61 Biopolis Dr., Singapore 138673.

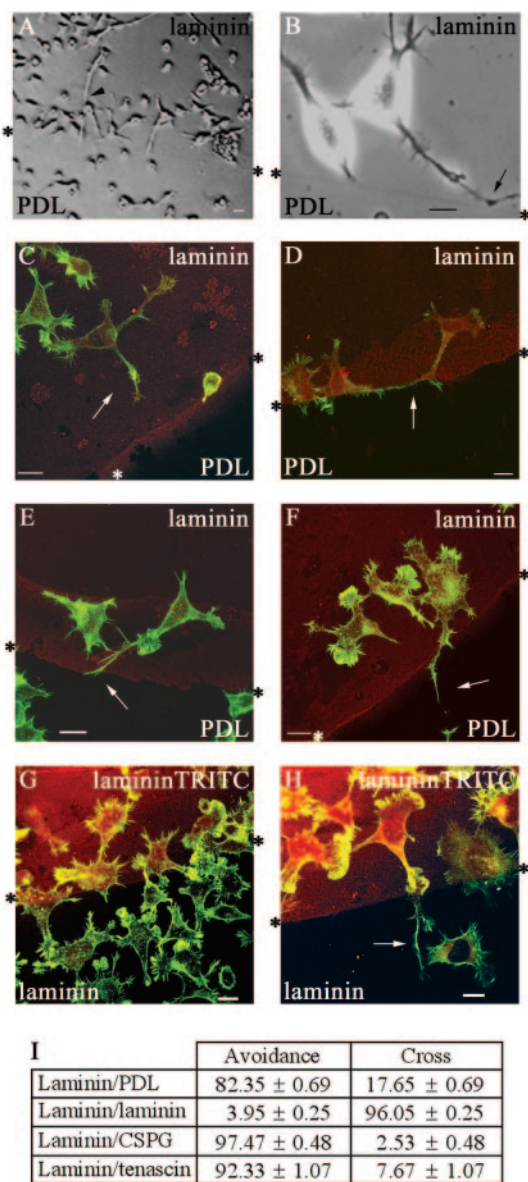


FIG. 1. N1E-115 neuroblastoma cells are responsive to signaling differences at a boundary. (A and B) Phase-contrast images of serum-starved cells at a laminin/PDL boundary. (A) Cells accumulated on the laminin side of the boundary and at the boundary have shorter neurites than those further away. (B) Neurite has begun to turn away from PDL (arrow), avoiding crossing from laminin. \*, boundary interface. (C to F) Fixed cells were stained with phalloidin (green) and laminin premixed with TRITC (red) to visualize the boundary interface. (C) Cell with shortened neurite (arrow) at laminin/PDL boundary—Stop category (D) Cell with neurite changing direction (arrow) at laminin/PDL boundary—Turn category. (E.) Cell with neurite containing long filopodia at its distal end (arrow), splaying out with a sidestepping morphology to avoid crossing PDL—Turn category. (F) Cell with neurite that has crossed (arrow) from laminin onto PDL—Cross category. (G and H) Cells at laminin-laminin-TRITC boundary remain in sharp focus, suggesting that laminin is not causing a ridge. In panel H a neurite that has crossed is indicated by an arrow. Cells were stained with phalloidin (green), and a secondary coat of laminin was mixed with TRITC dye (red). Scale bar = 20 μm in these and all subsequent figures. (I) Analysis of neurites that avoid crossing or cross the boundary between laminin and another substrate. The results are for three independent experiments (n = 6; 6 coverslips containing one boundary each) in all experiments except for laminin-laminin-TRITC, where

primary neuronal cells, for example, those derived from the hippocampus (8) or DRG, N1E-115 cells show no predisposition to produce outgrowth and therefore better mimic regenerating CNS neurons, which have only a low intrinsic ability to regenerate their axons (9, 10). N1E-115 cells will undergo differentiation and neurite outgrowth on withdrawal of serum (1). They are capable of responding to guidance cues; for example, their neurites will turn towards a source of ACh (20), a positive guidance response first demonstrated in spinal neurons of *Xenopus* (54). The response is dependent on activation of Cdc42 and Rac1 GTPases. The cells are easy to transfect, providing a large population where the effects of Rho GTPases or their effectors can be subjected to quantitative analysis. In this study, outgrowth of neurites from N1E-115 cells was induced through serum withdrawal or treatment with various agents. The effects of various components of the Rho GTPase signaling pathways on guidance behavior at boundaries of either CSPG or tenascin were analyzed. Serum withdrawal or RhoA inhibition promoted outgrowth of neurites that were able to avoid the repulsive surfaces. In serum-starved cells, this avoidance response could be overcome by introduction of various PAK derivatives, implicating PAK action in the negative guidance response.

MATERIALS AND METHODS

**Materials.** CSPG, tenascin, and their antibodies were from Chemicon. The peptide delivery system was BioPorter from Gene Therapy Systems (supplied by Q-Biogene, United Kingdom). Laminin was from ICN Flow; all other tissue culture reagents were from Life Technologies. Tetramethyl rhodamine isothiocyanate (TRITC) dye, used to mark the laminin, was from Sigma. PAK isoform antibodies were from Santa Cruz. Vinculin antibody was from Sigma; the laminin antibody was from Polyscience. The blocking peptides were from Santa Cruz and Jerini Germany.

**Cell culture.** N1E-115 cells were grown in Dulbecco's modified Eagle medium (DMEM) with 0.11g/liter sodium pyruvate, 4.5 g/liter D-glucose, and 580 mg/liter L-glutamine (Life Technologies). This medium was supplemented by adding 10% fetal calf serum (FCS) and 1% antibiotic/antimycotic solution (AB/AM) containing penicillin (10,000 U/ml), streptomycin (10,000 μg/ml), and amphotericin (25 μg/ml) (Life Technologies) as described previously (20, 40).

**Microscopy.** Phase images were taken of cells grown on chamber slides on a heated stage (37°C) in an atmosphere of humidified air and 5% CO<sub>2</sub>. Cells were video recorded using an Axiovert 135 microscope, Palmix TM-6CN video camera, and Sony-u-matic V0-5800 PS video recorder. Individual images were captured using Adobe Premier software and manipulated with Adobe Photoshop. Confocal microscopy was carried out using an LSM 410 Zeiss scanning microscope with three single-line lasers at 488 nM (argon), 543 nM, and 633 nM (HeNe).

**In situ localization.** For in situ analysis, primary and secondary antibodies were used at a 1:100 dilution. The PAK antibodies, all from Santa Cruz, were as follows: αPAK N20, βPAK N19, and γPAK N19. Cells were fixed with 4% paraformaldehyde in phosphate-buffered saline (PBS) for 10 min at room temperature (RT), washed with PBS two times for 10 min, permeabilized for 1 min in 0.5% Triton X-100 in PBS, and then blocked with 3% bovine serum albumin (BSA) in PBS for 15 min. The coverslips were then exposed to primary antibodies diluted 1/100 in 1% BSA in PBS and incubated at 37°C for 2 h in a humid chamber. Cells on coverslips were then washed in PBS twice for 10 min. Secondary antibodies diluted in 1% BSA in PBS and F-actin were stained with rhodamine-conjugated phalloidin (0.1 μg/ml; Sigma) and incubated with coverslips for 1 h in a dark humid chamber. Finally, coverslips were washed twice for 10 min in PBS and mounted in Immuno-Flore (ICN Flow). The slides were

n = 10. Standard errors of the means are shown here and in subsequent figures. For each condition in this and subsequent figures, the numbers of cells analyzed were from 139 to 1,310, with the average number being 530 cells.

allowed to set overnight before viewing with a Zeiss Axiovert microscope and a Zeiss LSM 410 confocal microscope.

**Cell guidance assays. (i) Permissive/attractive boundary.** Coverslips were first washed and sterilized and then coated in one of the following ways. The coverslips were covered with a solution of poly-D-lysine at 10  $\mu\text{g}/\text{ml}$  and incubated for 1 h at RT and then rinsed once with sterile water and allowed to air dry in a laminar flow hood before 30  $\mu\text{l}$  of laminin (10  $\mu\text{g}/\text{ml}$ ) was placed centrally and the coverslips incubated for 1 h at 37°C in a humid chamber to prevent evaporation and uneven application of the laminin. The coverslips were then rinsed twice in sterile water before being dried in the hood.

**(ii) Control boundary.** The coverslips were coated with laminin (10  $\mu\text{g}/\text{ml}$ ) for 1 h at RT and then rinsed in sterile water and left to dry. A second layer of laminin was applied as a 30- $\mu\text{l}$  drop mixed with 1  $\mu\text{g}/\text{ml}$  of TRITC label. Coverslips were left for 1 h at 37°C in a humidity chamber and then rinsed twice with sterile water and dried before use.

**(iii) Attractive/repulsive boundary.** Slides were coated with either tenascin at 10  $\mu\text{g}/\text{ml}$  or chondroitin sulfate proteoglycan (CSPG) at 5  $\mu\text{g}/\text{ml}$  for 1 h at 37°C in a humid chamber and then rinsed in sterile water and allowed to air dry before a 30- $\mu\text{l}$  drop of laminin (10  $\mu\text{g}/\text{ml}$ ) mixed with 1  $\mu\text{g}/\text{ml}$  of TRITC label was applied to the center of the coverslip and left for 1 h at 37°C in a humidity chamber before two rinses in sterile water and drying before use. This coating was also done in reverse with the laminin applied first and then the tenascin or the CSPG applied secondly. To ensure that the substrates were evenly applied and remained on the coverslips after attachment of cells, antibodies for tenascin, CSPG, or laminin were used to check the integrity of the substrates and to visualize the boundary on a sample of the coverslips; in this case the TRITC label was omitted.

Cells were then seeded onto the prepared coverslips at  $2 \times 10^5$  cells in 1 ml in a 35-mm petri dish in DMEM, 10% FCS, and 1% AB/AM. Cells were allowed to attach, the medium was then removed, and the coverslips were rinsed in serum-free medium and incubated overnight (16 h) in serum-free medium. The cells were fixed and stained to show the morphology of cells at the boundary.

**Time-lapse analysis of neurite behavior.** Cells were plated in Willco glass-bottom dishes coated with laminin-CSPG-TRITC or laminin-laminin-TRITC to create boundaries as described above. Cells were allowed to attach for 4 h. After withdrawal of serum and addition of Y-27632 (final concentration, 10  $\mu\text{M}$ ) to induce rapid outgrowth of neurites, the cells were placed in a mini-incubator mounted to a Bio-Rad Radiance 2000 confocal system. Cells were imaged over 2.5 h. Images were captured at 45-s intervals using a Nikon 40 $\times$  oil objective and were processed using Adobe Photoshop.

**Transient transfection.** Cells were harvested by gentle pipetting to remove attached cells and plated out at  $1.5 \times 10^5$  cells/ml in a 35-mm dish containing prepared coverslips and incubated overnight. The medium was then replaced with 1 ml of serum-free DMEM only and the cells incubated for 1 h at 37°C. Two hundred microliters of DMEM was placed into a sterile 1.5-ml Eppendorf tube, and 1  $\mu\text{g}$  of the plasmid DNA (in eukaryotic expression vector PXJ40) was added to each tube with 6  $\mu\text{l}$  of Lipofectamine 2000 (GIBCO), followed by gentle inverting and then incubation at RT for 45 min to allow the lipids to package the DNA. At the end of the incubation the mix was added to the dish containing the cells, and they were then incubated for 4 h at 37°C. After incubation the transfection mix was then removed and the cells rinsed with 1 ml of DMEM-5% FCS-1% AB/AM; 1 ml of the same medium was added, and the cells incubated for a further 16 h.

**Protein delivery system.** The BioPorter reagent was prepared according to the manufacturer's instructions. Cells were plated out at  $1.5 \times 10^5$  cells in a 35-mm dish containing prepared coverslips and incubated overnight. The protein or peptide of interest was diluted in 100  $\mu\text{l}$  PBS to give a final concentration of 10  $\mu\text{g}/\text{ml}$ , and 1  $\mu\text{l}$  of fluorescein isothiocyanate-labeled goat immunoglobulin G (IgG) was added to act as a marker. This mixture was added directly to the tube containing the BioPorter reagent, mixed by pipetting up and down two or three times, and then allowed to stand for 5 min. Cells were washed once with serum-free DMEM; 1 ml of serum-free DMEM was added to the tube containing the peptide and BioPorter mix and vortexed gently before being added to the cells. The cells were incubated for 4 h at 37°C. After incubation the cells were then incubated for a further 2 h in 5% FCS-DMEM or serum-free DMEM for cells undergoing a substrate guidance assay. The cells were then fixed and stained.

**Immunoblot analysis of PAK isoforms.** N1E-115 cells were harvested after growing in 10% FCS in DMEM. The supernatants of lysed, sonicated cells were subjected to 10% sodium dodecyl sulfate-polyacrylamide gel electrophoresis analysis. Gels containing separated proteins were blotted onto nitrocellulose filters. The filters were blocked in 5% milk powder (Marvel)-PBS-0.1% Tween 20, washed with PBS, and incubated with the relevant primary (PAK) antibody (1/1,000 dilution) in 1% milk-PBS-0.1% Tween 20 for 1 h at RT. The primary antibody was washed off with PBS-0.1% Tween 20 (PBST), and secondary

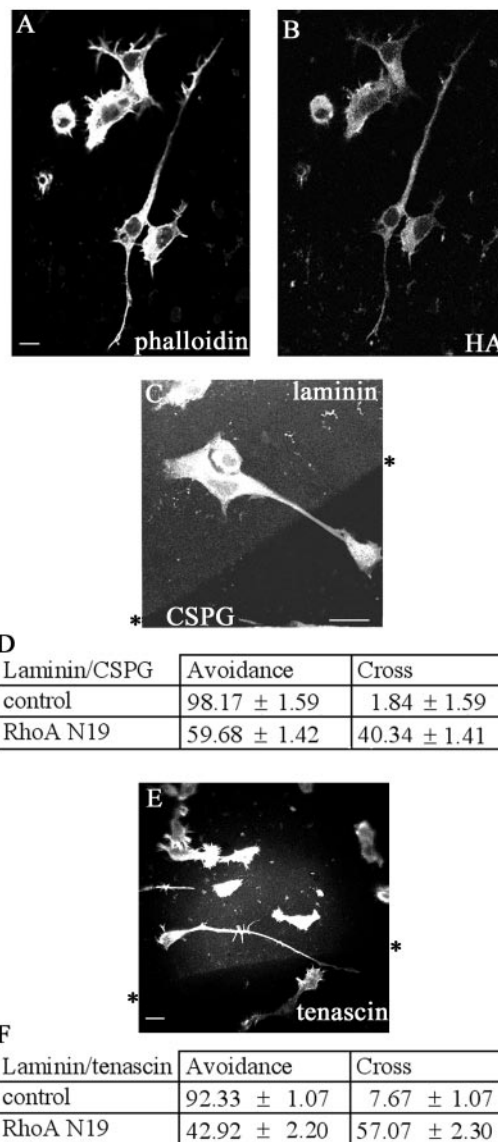


FIG. 2. Transfection with RhoA N19 induces outgrowth of neurites with increased numbers crossing from laminin onto CSPG or tenascin. (A) RhoA N19-transfected cell on laminin, stained with phalloidin. (B) RhoA N19-transfected cell stained with HA antibody. (C) Neurite of RhoA N19-transfected cell crossing from laminin onto CSPG, stained with phalloidin. (D) Analysis of increased neurite crossing from laminin onto CSPG by RhoA N19-transfected cells. Results are for three independent experiments ( $n = 6$  for controls [serum starvation and mock transfection treatment]) ( $n = 21$  for RhoA N19-transfected cells). (E) RhoA N19-transfected N1E-115 cell stained with phalloidin crossing from laminin onto tenascin. (F) Analysis of increased neurite crossing from laminin onto tenascin by RhoA N19-transfected cells. Results are for three independent experiments ( $n = 6$  for control and RhoA N19-transfected cells).

antibody (1/1,000 dilution) added. Filters were incubated for 1 h, washed in PBST, blot dried, and then developed using ECL reagents (Amersham Pharmacia Biotech). For immunoblots, primary and secondary antibodies were used at a 1/1,000 dilution.

**Assay of Rac1-GTP levels.** N1E-115 cells grown in 5% FCS on plastic, laminin, or CSPG were transfected with HA-RhoA N19, as described above. Cell extracts from mock- and RhoA N19-transfected cells were assayed for their Rac-GTP content using glutathione *S*-transferase (GST)/PAK-CRIB constructs and Rac1 antibodies essentially as described previously (4).

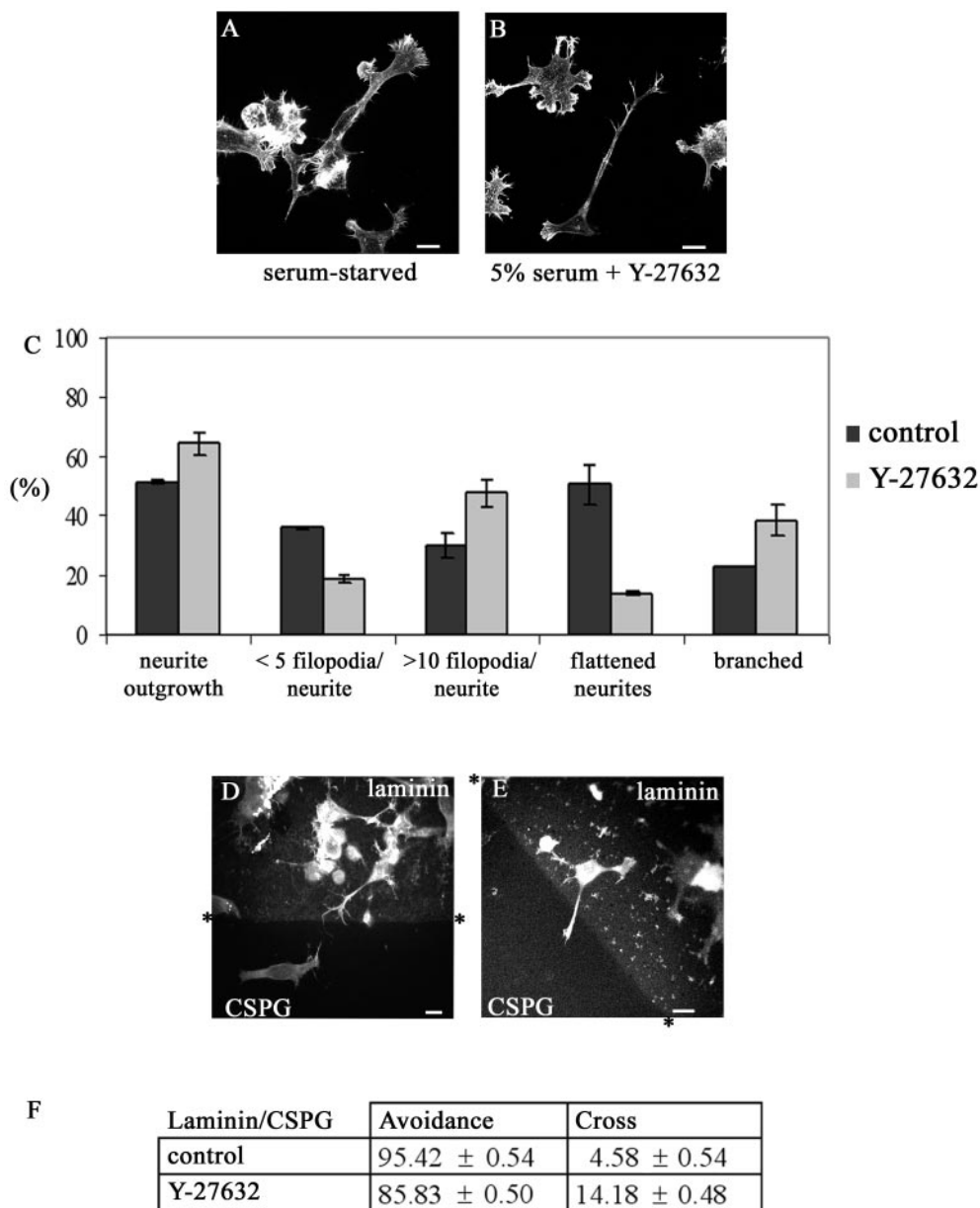


FIG. 3. Effects of the ROK inhibitor Y-27632 on neurite outgrowth and guidance. (A) Serum-starved cells showing outgrowth but with flattened neurites and areas of lamellipodial spreading. (B) Cells grown in 5% FCS-DMEM with added Y-27632 (10  $\mu$ M) contain neurites that are spread less, with terminal actin-dense projections, more branched, and/or contain actin-dense projections along the neurite shaft. (C) Y-27632 treatment induces neurite outgrowth in 5% FCS. Results are for three independent experiments ( $n = 6$ ). Error bars denote standard errors of the means in this and subsequent graphs. Serum-starved NIE-115 cells rarely have branched neurites. With treatment using different agents, outgrowing neurites become more branched. The categories are as follows: branched neurites, two branches or more per neurite; flattened neurites, those with lamella and generally 1/3 to 1/4 of cell body width (normally neurites are 1/5 cell body width) (filopodium values refer to numbers of filopodia on neurite shaft). (D and E) Cells at laminin/CSPG boundary after Y-27632 treatment. Asterisks indicate boundary interfaces. (D) Cell with a neurite avoiding crossing onto the CSPG through sidestepping. (E) Cell with a neurite crossing onto CSPG from laminin. Cells and boundary stained as in Fig. 1. (F) Treatment with Y-27632 for 6 h promotes substantial neurite outgrowth in the presence of 5% serum and slightly affects the negative guidance response. Results are for three independent experiments ( $n = 8$  for control;  $n = 14$  for Y-27632-treated cells).

**Effect of Rac1 N17 expression on cell morphology.** NIE-115 cells were grown in 10% FCS either on laminin or CSPG for 4 h overnight. Cells were then transfected with HA/Rac1 N17 as described above. The morphologies of mock and Rac1 N17-transfected cells were examined after staining with phalloidin or hemagglutinin (HA) antibody as described above. Cells were categorized into those that were contracted (a), showing neurite outgrowth (b), flattened (c), or elongated (d).

**Statistical analysis.** Data are expressed as mean values from three independent experiments; error bars represent standard errors of the mean values. The  $n$  values refer to the numbers of coverslips, each containing a boundary, subjected to analysis. The neurites analyzed were all within a 40- $\mu$ m strip along the laminin side of the boundary in each coverslip, the average number analyzed being  $\sim 50$ . Values from the control and experimental groups were compared using the Mann-Whitney U test with a  $P$  value of  $< 0.05$  considered significant.

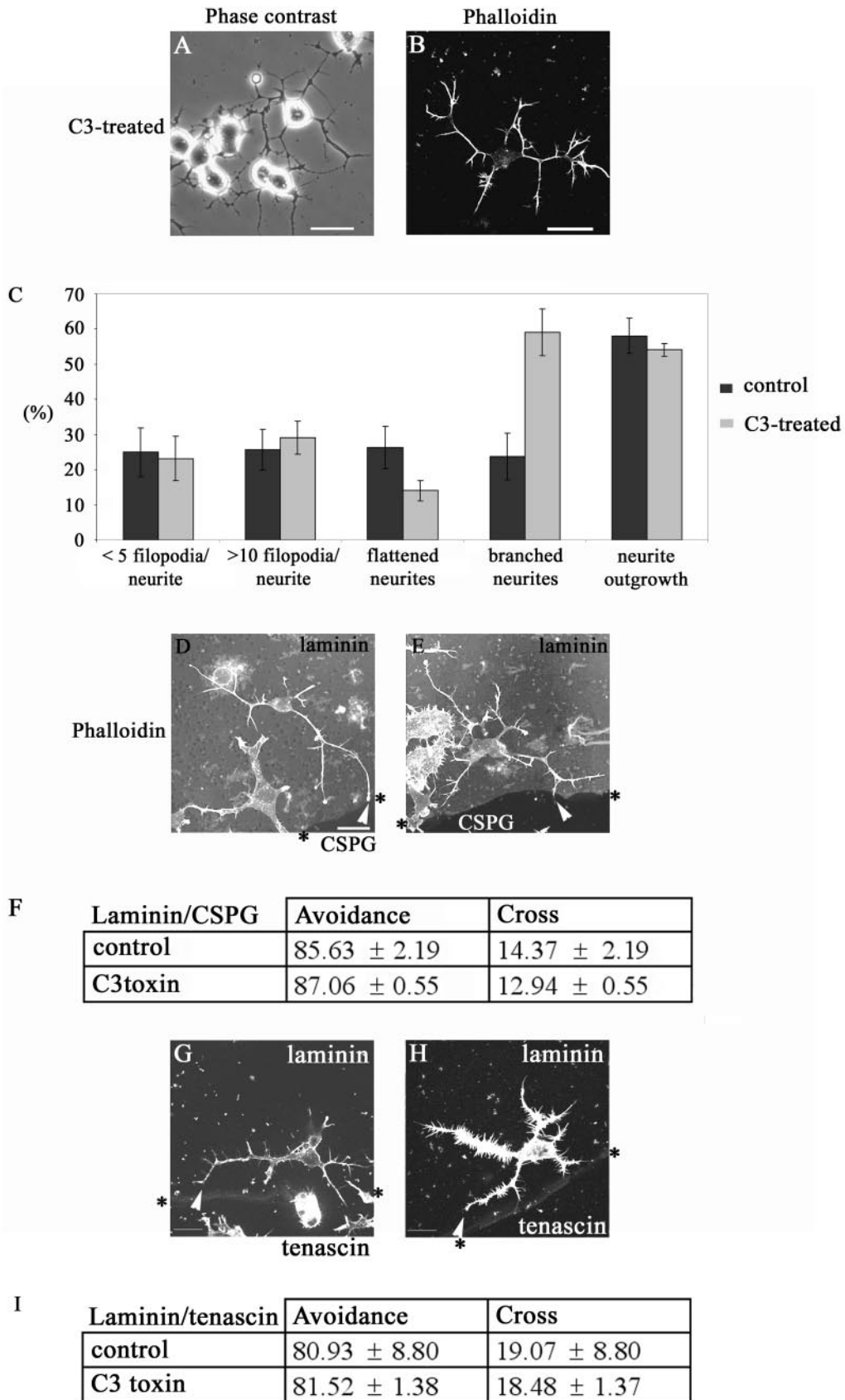


FIG. 4. C3 toxin promotes outgrowth of neurites that display a negative guidance response. (A) Phase-contrast image and (B) phalloidin staining of cells in 5% serum after BioPorter delivery of C3 toxin, showing neurite outgrowth. (C) Morphology of neurites induced by C3 toxin

## RESULTS

**Response of N1E-115 neuroblastoma cells to negative guidance signals.** We previously observed that N1E-115 neuroblastoma cells directed their neurites towards a source of ACh, supplied as a gradient, only when first plated on laminin, but not on culture dishes alone (20). This suggests that these cells not only respond to soluble guidance clues but also to the nature of the substrate.

To determine how neurite behavior was affected by favorable and unfavorable substrates, cells were seeded onto coverslips with discrete coatings of laminin and poly-D-lysine (PDL) and allowed to attach. The cells were then serum starved to cause differentiation. Cells close to the boundary between the two substrates were viewed with an inverted microscope fitted with a CO<sub>2</sub>-controlled humidified chamber and a heated stage. Phase analysis showed that cells accumulated in a strip of approximately 300 μm on the laminin side of the boundary. Neurites in this strip tended to be shorter, suggesting that growth may have terminated before the neurites reached full length, as serum-starved N1E-115 cells generally possess neurites in excess of two cell body lengths (Fig. 1A). In cells with neurites and growth cones at the boundary, the filopodia on the growth cone were observed occasionally to make contact with the other substrate. Phase analysis of cells with neurites in this strip showed them to have specific morphologies, which may well reflect the avoidance response to PDL. Neurites close to the boundary were often shorter than neurites further away, suggesting a premature termination (Fig. 1A). In other cases, filopodia often appeared to sense the boundary region, and on occasions the growth cone splayed out with numerous projections before the whole neurite grew and turned away from the boundary (Fig. 1B, arrow).

The assay relies on the ability of cells to produce outgrowth while undergoing guidance decision making over a time course of around 18 h. Therefore, to study the morphology of the cells at the boundary in more detail and in greater numbers, cells were fixed and stained with phalloidin to visualize F-actin and an anti-laminin antibody was used to detect the laminin and delineate the boundary. Neurites within a 40-μm strip along the laminin side of the boundary were analyzed; this would include neurites that had been able to sense the boundary and retracted. The fixed and stained cells at the boundary were compared with phase images of the live cells to determine their corresponding morphologies. Based on this comparison, their morphologies were then categorized. Neurites were scored when greater than one cell body length as they generally stained positively for neurofilament; most serum-starved neurites were greater than two cell body lengths away from the boundary (Fig. 1A).

The categories were as follows. (i) Stop—the neurite had

stopped at or very close to the boundary (Fig. 1C). (ii) Turn—the neurite showed a marked deviation in direction, suggesting that it had initiated a turn as seen in the phase analysis (Fig. 1D) or the neurite had splayed to form numerous projections or a zigzag shape along the boundary, possibly sidestepping before turning (Fig. 1E). (iii) Cross—the neurite had crossed from one substrate to the other (Fig. 1F).

The first two categories are indicative of cells that may be responding to the (repulsive) signals from the other substrate and thus avoid crossing. The third category is indicative of cells not responsive to the signals from the substrate for various reasons or of cells where the present and newly encountered substrates evoke similar responses.

The first two categories were aggregated and scored as neurites avoiding crossing and compared with those that crossed the boundary (Fig. 1I). A large majority (83%) of cells plated on the laminin substrate avoided crossing onto the PDL.

To determine whether the cells were responsive to signaling differences between different substrates at a boundary or merely to an interface, experiments were repeated using “false” boundaries or two identical substrates. Cells encountering either a “false” boundary or a boundary between the same substrate should be subjected to identical signals and therefore be expected not to show any avoidance behavior. False boundaries were created by using a fine marker to mark a circle on the coverslips. To demonstrate that laminin was not causing a ridge when used to cover another substrate, coverslips were coated with laminin and a central drop of laminin mixed with TRITC dye to visualize the boundary was then applied. Cells were seeded and serum starved and analyzed as before (Fig. 1G and H). At a laminin–laminin–TRITC boundary, cells showed very little avoidance behavior, with the majority crossing (Fig. 1I). Cells crossing or on the boundary remained in sharp focus, indicating that the laminin did not cause a significant ridge (Fig. 1G and H). N1E-115 cells thus have the ability to respond to signals from differing substrates, and this results in the cells growing in a directed manner away from a less favorable substrate.

To ascertain if the N1E-115 cells would respond to signals from more physiologically relevant substrates, especially those associated with damaged areas of the nervous system, the guidance assay was repeated using a boundary between laminin (as the permissive substrate) and CSPG or tenascin (as the repulsive substrate). Cells showed a marked repulsion response when encountering CSPG, with >97% of neurites avoiding crossing onto CSPG. Only 2% crossed, as compared with about 17% crossing from laminin onto PDL. Clearly, CSPG elicited a greater repulsive response from N1E-115 cells than PDL, with the vast majority of the cells showing avoidance. As with

---

or control (serum starvation and BioPorter-delivered IgG). Results are for three independent experiments ( $n = 6$  for control and  $n = 8$  for C3 toxin-treated cells). The categories of neurite morphology are as defined in the legend to Fig. 3. (D) Neurite of C3 toxin-treated cell is able to avoid crossing from laminin onto the CSPG. The arrowhead points to the termini at branched neurite, with a rounded “club-like” appearance, suggestive of neurite withdrawal and collapse. (E) As for panel D but with the neurite of C3 toxin-treated cell turning at a laminin/CSPG interface (arrowhead). (F) Avoidance of CSPG by neurites is retained in C3 toxin-treated cells. Results are for three independent experiments ( $n = 10$  for control,  $n = 19$  for C3 toxin-treated cells). (G and H) C3 toxin-treated cells with neurites turning at laminin/tenascin boundary (arrowheads). (I) Avoidance of tenascin by neurites is retained in C3 toxin-treated cells compared with the control (serum starvation and BioPorter-delivered IgG). Results are for three independent experiments ( $n = 8$  for control;  $n = 13$  for C3 toxin-treated cells).

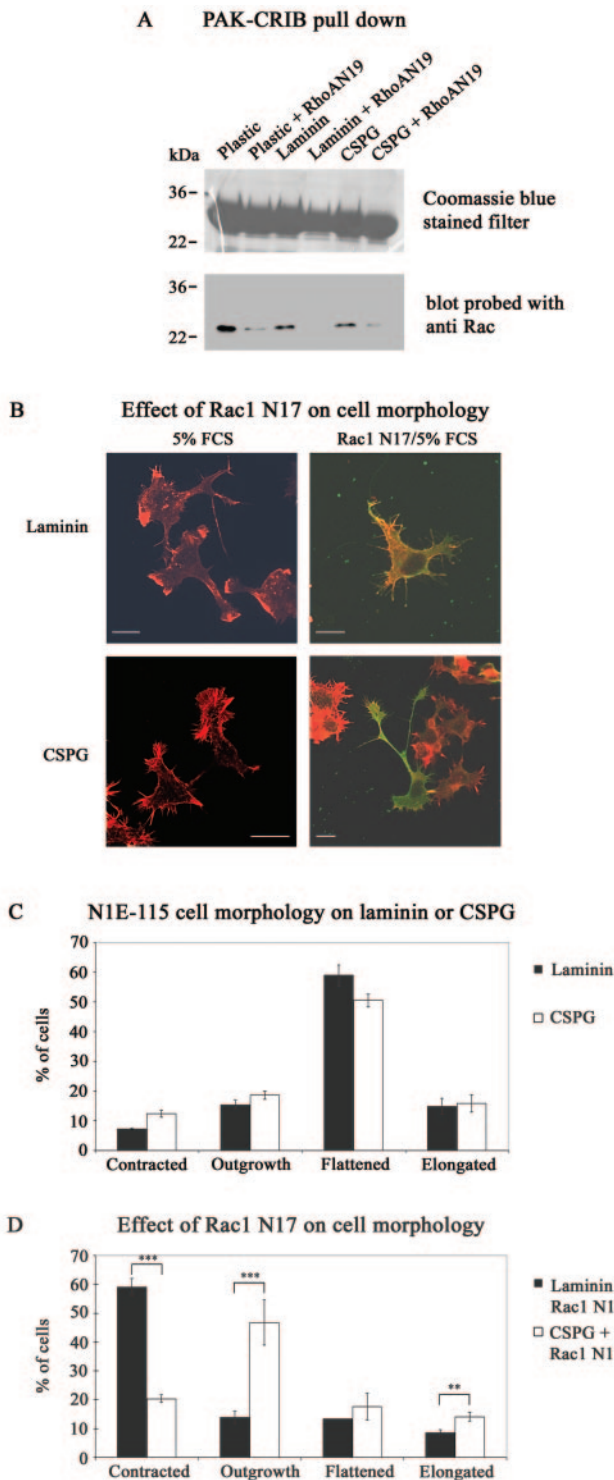


**FIG. 5.** Rac1 activation is affected by RhoA N19 and is involved in neurite outgrowth on CSPG. (A) N1E-115 cells grown in 5% FCS on plastic, laminin, or CSPG were transfected with HA-RhoA N19. The relative content of Rac-GTP was analyzed using PAK-CRIB pull-down assays and Rac antibodies. In all cases, RhoA N19 decreased Rac-GTP content. The upper gel contains the GST/CRIB fragment; the lower gel is an immunoblot of Rac. The results shown are typical of four independent assays. (B) Effect of Rac1 N17 on cell morphology. N1E-115 cells grown in 5% FCS either on laminin or CSPG were transfected with HA/Rac1 N17. Cells were stained with phalloidin (red) or anti-HA (green). Expression of Rac1 N17 promotes neurite outgrowth

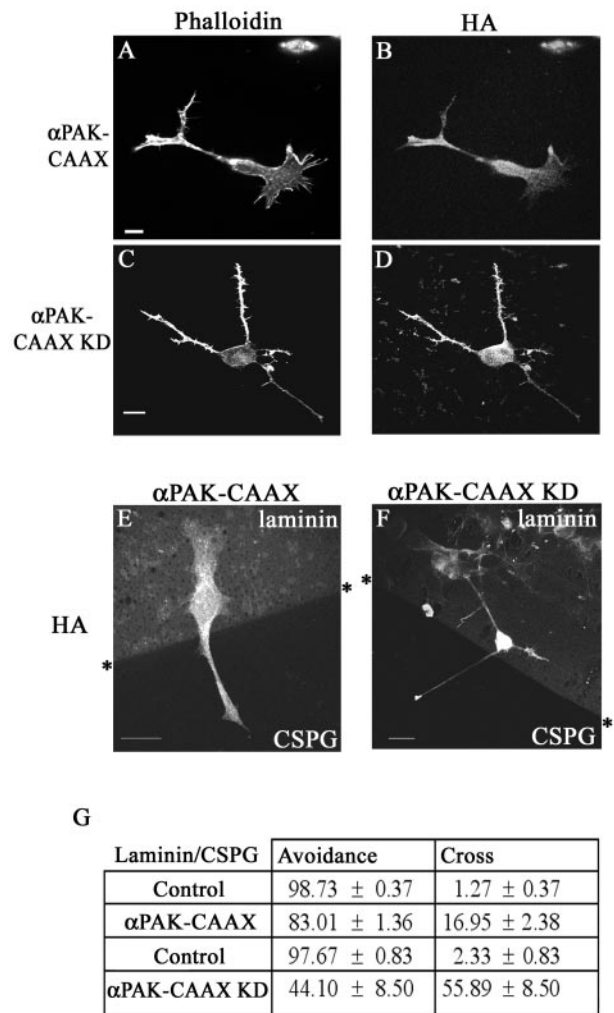


**FIG. 6.** Effects of membrane-targeted PAK on the negative guidance response. Neurite outgrowth in cells transfected with αPAK-CAAX (A and B) or αPAK-CAAX KD (C and D). Stained with phalloidin (A and C) or anti-HA (B and D). Neurites of cells transfected with αPAK-CAAX (E) or with αPAK-CAAX KD (F) crossing a laminin/CSPG boundary. HA-tagged cells are shown. (G) Neurites of cells transfected with either PAK construct have an increased ability to cross from laminin onto CSPG. Results are for three independent experiments ( $n = 6$  for controls,  $n = 8$  for αPAK-CAAX-transfected cells, and  $n = 14$  for αPAK-CAAX KD-transfected cells).

CSPG, a large majority of cells (92%) avoided crossing onto a tenascin substrate (Fig. 11).

**RhoA N19 and neurite guidance.** RhoA activation has been implicated in the regulation of negative guidance signals, involving ephrin A5-induced collapse of retinal growth cones (50). We then investigated the role of RhoA-mediated signaling in the negative guidance response using the dominant neg-

in cells grown on CSPG (see cell in bottom right panel). (C) Analysis of morphology of cells grown on laminin or CSPG. Note occurrence of predominantly flattened cells. (D) Analysis of effect of Rac1 N17 on cell morphology. Note enhanced neurite outgrowth on cells grown on CSPG but not on laminin. Error bars represent standard errors of the means. \*\*,  $P < 0.01$ ; \*\*\*,  $P < 0.001$ .

ative RhoA N19 mutant. Neurite outgrowth was promoted in cells transiently transfected with RhoA N19; the neurites were long, straight, and predominantly unbranched (Fig. 2A and B). Cells plated on coverslips containing either a laminin/CSPG or a laminin/tenascin boundary were then transiently transfected with RhoA N19 and allowed to express for 18 h. The cells were fixed and stained for phalloidin and HA antibody to detect the transfected cells; the laminin boundary was detected with laminin antibody (Fig. 2C).

Whereas the vast majority (98%) of the serum-starved mock-transfected control cells contained neurites that did not cross from the laminin onto CSPG, only about half of cells transfected with RhoA N19 avoided crossing (Fig. 2E). RhoA N19-transfected cells also showed a marked decrease in their avoidance behavior towards tenascin, with less than half (43%) avoiding crossing (Fig. 2D and F).

**ROK inhibition and neurite guidance.** We next investigated whether this guidance response involved the Rho kinase ROK, which causes neurite collapse (14, 18). ROK activity is inhibited by the kinase inhibitor Y-27632 (18, 25), which is able to prevent lysophosphatidic acid-induced collapse of neurites or to induce neurite outgrowth in N1E-115 cells in the presence of serum (14). Serum-starved cells contained flattened neurites and areas of lamellipodial spreading. Treatment of cells with Y-27632 (10  $\mu$ M in 5% FCS) resulted in outgrowth of neurites that were more branched, with more filopodia on the neurite shaft, and less flattened compared with serum-starved controls (Fig. 3A to C).

The effect of Y-27632 on the guidance of N1E-115 cells at a laminin/CSPG boundary was then examined. Cells were plated onto a laminin/CSPG boundary as described above. Y-27632 in 5% serum was added, and cells incubated for 6 h before fixing and staining. The results are shown in Fig. 3D, E, and F. In the case of serum-starved cells, 95% of the neurites were able to avoid crossing onto CSPG. Treatment with Y-27632 resulted in only a slight decrease in the number of neurites that avoided crossing onto CSPG (86%). Since the ROK inhibitor Y-27632 caused only a minor disruption in guidance when compared with RhoA N19, this may indicate that other Rho effectors or another pathway is involved.

**Rho inhibition by C3 toxin and neurite guidance.** To further understand the role of Rho signaling, we next used the *Clostridium botulinum* toxin C3, which specifically inhibits the action of Rho by ADP-ribosylation (41). C3 toxin *in vivo* is a more potent blocker of Rho function than RhoA N19 (45). Because C3 toxin is not cell permeable, the BioPorter system was used to provide its effective delivery into N1E-115 cells. After plating of the cells, 5  $\mu$ g of C3 toxin and the BioPorter reagent were added. Six hours later, the cells were fixed and stained to determine the number of cells with neurites more than one cell body length and the type of outgrowth produced (Fig. 4A to C). The effect on the cells was very similar to that previously seen on C3 toxin injection (20). The morphology produced was that of multiple branched neurites, and the cell body was more contracted compared with serum-starved control cells.

There was no difference in the response to a laminin/CSPG boundary between the control serum-starved and C3 toxin-treated cells (Fig. 4D, E, and F). Nor was the ability of cells to guide at a laminin/tenascin boundary affected by the treatment

with C3 toxin (Fig. 4G, H, and I). These results with the C3 toxin indicate that inhibition of Rho leads to outgrowth of neurites that are able to avoid crossing on to repulsive substrates like CSPG and tenascin.

**Rac, PAK, and neurite guidance.** The exact role of RhoA N19 is uncertain; it may well affect activation of GTPases other than Rho. A Rac1-mediated collapse pathway has been implicated in other repulsive signaling, e.g., that involving Sema3A (16, 21, 49). Because its dominant negative N17 mutant blocks the neurite outgrowth (20, 40) essential for our assay, Rac1 involvement in guidance could not be investigated directly. Nevertheless, we were able to show that Rac1 activation was affected by RhoA N19. In cells plated either on plastic, laminin, or CSPG, transfection with RhoA N19 resulted in decreased levels of Rac1-GTP within the cell (Fig. 5A). This suggested that the enhancement by RhoA N19 of neurite crossing onto CSPG (Fig. 2) could have occurred through its inhibition of Rac1 pathways. We then examined whether Rac1 N17 itself could promote neurite outgrowth of N1E-115 cells grown on CSPG. Many of the cells (~50%) plated on laminin or CSPG in 5% serum were flattened, with the rest equally distributed between those that were contracted, elongated, or showing neurite outgrowth (Fig. 5B and C). Under these conditions, a Rac- rather than Rho-type morphology predominated. Serum contains lysophosphatidic acid, which has been shown recently to activate both Rho and Rac pathways sequentially, with activation of the latter leading to inhibition of the former (48). On expressing Rac1 N17, the cells plated on laminin (Fig. 5B and D) had an altered morphological distribution, with most (~60%) now being contracted (Rho-type morphology) rather than flattened (12%). Expression of Rac1 N17 by cells plated on CSPG also resulted in an altered morphological distribution, but with many now showing neurite outgrowth (~45%) rather than being flattened (15%). Thus, with cells plated on CSPG but not on laminin, Rac1 inhibition promoted neurite outgrowth (see example in Fig. 5B, lower right panel).

Since Rac1 N17 is inimical to neurite outgrowth on laminin, we examined the role of its downstream effector PAK on the negative guidance response. Transfection with  $\alpha$ PAK does not lead to neurite outgrowth; PAK is probably subject to stringent intracellular regulation since autoactivated PAK (mutated in the p21-binding domain) evokes massive morphological changes in cells (26). The latter observation precluded the use of non-p21-binding mutants of PAK. However, the  $\alpha$ PAK sequence modified to include the membrane-targeting sequence CAAX (26) promotes neurite outgrowth in PC12 cells (6). We then examined the effects of  $\alpha$ PAK-CAAX as well as its kinase-dead derivative,  $\alpha$ PAK-CAAX<sup>K298</sup> ( $\alpha$ PAK-CAAX KD). Cells transfected with  $\alpha$ PAK-CAAX typically possess long neurites that are occasionally branched and terminate with a small growth cone (Fig. 6A and B). Cells transfected with  $\alpha$ PAK-CAAX KD possess spindly neurites with numerous filopodia along their length, and they have a tapered appearance (Fig. 6C and D). Cells were then plated onto a laminin/CSPG boundary, transiently transfected with  $\alpha$ PAK-CAAX or  $\alpha$ PAK-CAAX KD, and allowed to express for 18 h. The transfected cells were detected with an anti-HA antibody; the laminin boundary was detected as before, and the results are shown in Fig. 6E, F, and G.

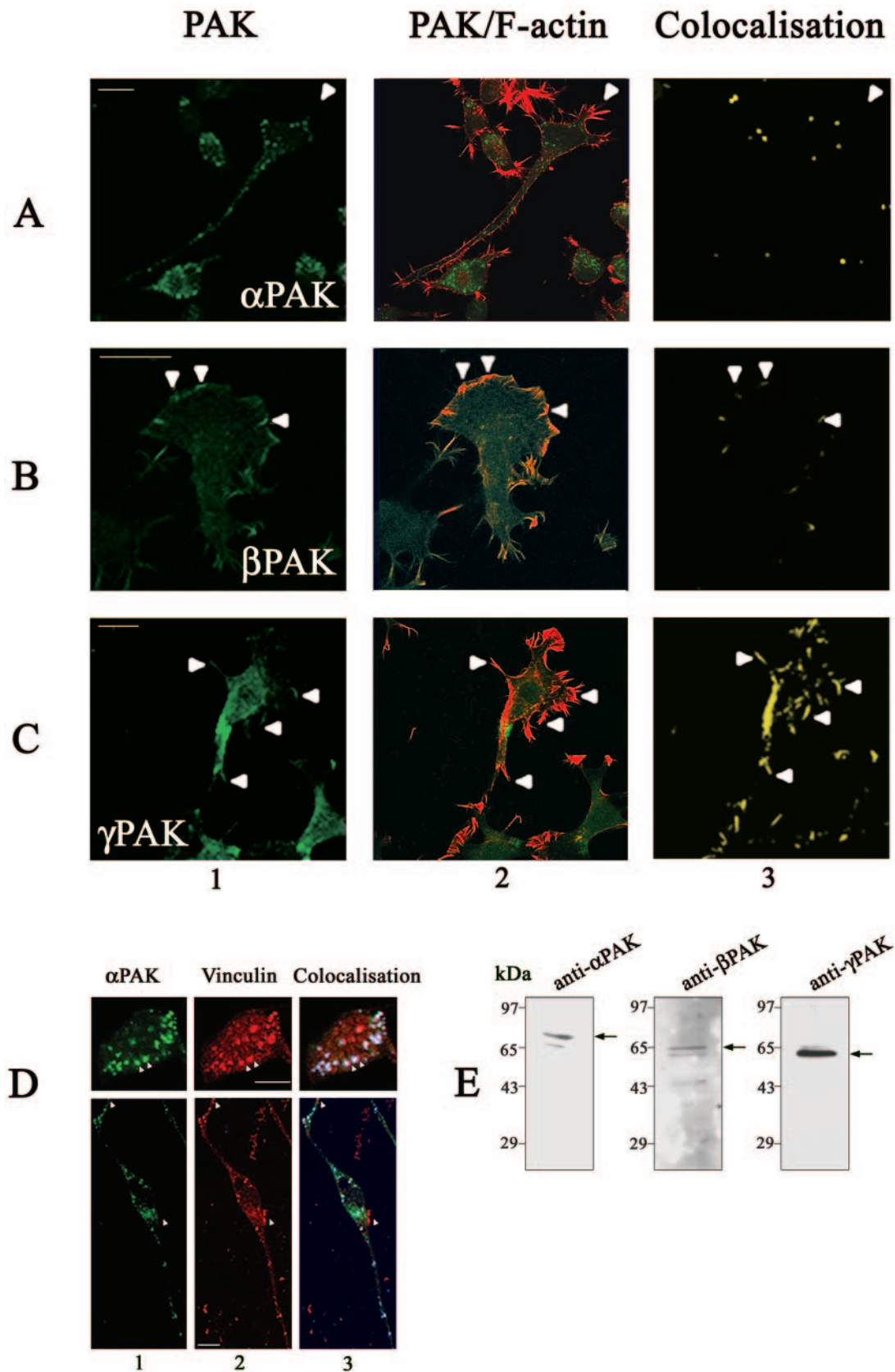


FIG. 7. Endogenous isoforms of PAK locate to distinctive regions of N1E-115 cells and are associated with F-actin structures. Serum-starved N1E-115 cells were stained with antibodies to (A)  $\alpha$ PAK, (B)  $\beta$ PAK, or (C)  $\gamma$ PAK (panel 1, green) and costained with phalloidin (panel 2, red). Panel 3 shows areas of colocalization (yellow) between the different PAK isoforms and F-actin.  $\alpha$ PAK is localized mainly in central clusters and

Cells transfected with  $\alpha$ PAK-CAAX or its kinase-dead derivative displayed a marked change in their avoidance behavior. Whereas in control cells, only 2% of neurites crossed onto the CSPG from laminin, in  $\alpha$ PAK-CAAX- and  $\alpha$ PAK-CAAX KD-transfected cells the corresponding numbers were 17% and 56%, respectively. A series of similar experiments with cells transfected with other Cdc42-binding effectors such as N-WASP and IRS-58 (2, 12) showed that they elicited no increase in the numbers crossing (data not shown). These results indicate that membrane-targeted PAK can overcome the negative guidance response, with the kinase-dead form being more effective.

**PAK isoforms in neurite outgrowth and actin structures.** We then investigated which of the PAK isoforms might be involved in the negative guidance response. Expression of all three endogenous PAK isoforms in N1E-115 cells was confirmed by immunoblotting using isoform-specific antibodies. The antibodies for  $\alpha$ PAK,  $\beta$ PAK, and  $\gamma$  PAK separately predominantly recognized 68-kDa, 65-kDa, and 62-kDa proteins, respectively, in cell extracts (Fig. 7E). These molecular masses correspond to those of the different PAK isoforms. We also examined the localization of endogenous PAK isoforms and their relationship to F-actin structures. Cells were plated onto laminin-coated coverslips and serum starved to induce outgrowth. Each PAK isoform showed a preferential distribution at distinct sites where they colocalized with F-actin.  $\alpha$ PAK was found predominantly in the center of cells in small clusters and along the neurite shaft but not associated with filopodia or lamellipodia (Fig. 7A).  $\beta$ PAK was found mainly in areas with lamellipodia and membrane ruffling; the staining in filopodium-like structures was more diffuse and not as enriched as in the ruffling areas (Fig. 7B).  $\gamma$ PAK was found mainly in areas of filopodium activity and some stabilized filopodia and not in areas of membrane ruffling (Fig. 7C).

The  $\alpha$ PAK-containing clusters in cells growing in 10% FCS were associated with vinculin, a focal complex marker (Fig. 7D). Differentiation and neurite outgrowth through serum withdrawal resulted in a substantial decrease in these clusters (Fig. 7D). The  $\alpha$ PAK-containing clusters thus resemble RhoA-type focal adhesion complexes that are associated with stress fibers in fibroblasts.

**Effects of PAK peptides on neurite outgrowth and morphology.** We then used isoform-specific PAK peptides to investigate their effects on the outgrowth of neurites and the negative guidance response. The PAK peptides selected were small sequences spanning the divergent N terminus of each isoform. They each contained a polyproline-rich segment essential for binding to Nck (53) and a small flanking region:  $\alpha$ PAK, SNNGLDIQDKPPAPPMRNTS ( $\alpha$ P2 peptide);  $\beta$ PAK, SDSLDNEEKPPAPPLRMNSNN ( $\beta$ P2 peptide);  $\gamma$ PAK, SDNGELEDKPPAPVRMSSTI ( $\gamma$ P2 peptide).

The individual peptides were delivered, using BioPorter with marker IgG, to cells plated onto laminin-coated coverslips that were then incubated at 37°C for 6 h before staining with phalloidin, all under serum-free conditions. Serum-starved control cells were treated with BioPorter containing IgG. Staining for the codelivered IgG marker identified the relevant cells. None of the PAK peptides blocked the neurite outgrowth caused by serum starvation, with the  $\beta$ P2 peptide slightly increasing the number of cells with neurites (Fig. 8A). The morphology of the neurites of peptide-containing cells was also compared with that of control cells (Fig. 8B and C).  $\alpha$ P2 peptide had no discernible effect.  $\beta$ P2 peptide induced production of more filopodia on the neurite shaft and on the growth cone, giving rise to a “hairy” appearance to the cells; more branched neurites were also seen.  $\gamma$ P2 peptide-containing cells had neurites that were smoother or more flattened and with typically five or less filopodia per cell.

**Effect of N-terminal PAK peptides on the guidance response.** The peptides were then delivered to cells plated on coverslips containing a laminin/CSPG boundary under serum-free conditions. After 6 h to induce neurite outgrowth, the cells were fixed and stained. The neurites of the cells containing the PAK peptides all stained positively for F-actin and for neurofilament. The morphology and response of these cells are shown in Fig. 9A to D. The response is quantified in Fig. 9E, where neurites that showed avoidance behavior were subcategorized as those showing “stop” or “turn” responses.

The neurites from cells containing the  $\gamma$ P2 peptide showed a substantial change in their ability to respond to a laminin/CSPG boundary, with two-thirds now crossing onto the CSPG. The increase in numbers of neurites that crossed appeared largely to be derived from those that normally would have avoided crossing by turning away from the boundary. The presence of the  $\alpha$ P2 peptide did not affect the numbers crossing, while that of the  $\beta$ P2 peptide elicited very much less of an effect than the  $\gamma$ P2 peptide.

As the  $\gamma$ P2 peptide appeared to affect the crossing ability of neurites that would normally have turned away from the repulsive substrate, we reexamined the effects of those agents most effective in disrupting guidance, this time subdividing those neurites previously within the avoidance category into the stop and turn categories. Figure 10 is a time-lapse analysis showing neurites stopping at a laminin-CSPG boundary (Fig. 10A) or crossing a laminin-laminin boundary (Fig. 10B) within a 2.5-h period. In this illustration of the stop category, neurite outgrowth has been accelerated by serum withdrawal combined with Y-27632 treatment to facilitate the analysis of neurite dynamics.

In our reexamination of the avoidance category, we noted that cells that were not or were little affected in their negative guidance response by the presence of inhibitors (C3 toxin and

---

along neurite shafts and absent from filopodia (arrowheads, A).  $\beta$ PAK occurs in lamellipodium/membrane ruffles (arrowheads, B) and  $\gamma$ PAK mainly in filopodia (arrowheads, C). (D) Cells grown in 10% FCS were costained with antibodies to  $\alpha$ PAK (upper panel 1, green) or vinculin (upper panel 2, red). Upper panel 3 shows colocalization (blue) of  $\alpha$ PAK and vinculin in clusters resembling focal adhesions (two indicated by arrowhead). In the serum-starved cell (lower panels), clusters are smaller and centrally located; they appear in areas of flattening but not those enriched in filopodia or lamellipodia (arrowheads). (E)  $\alpha$ -,  $\beta$ -, and  $\gamma$ PAK expression in N1E-115 cells. Cellular proteins separated by sodium dodecyl sulfate-polyacrylamide gel electrophoresis were subjected to Western blot analysis using antibodies to  $\alpha$ PAK (62 kDa),  $\beta$ PAK (65 kDa), and  $\gamma$ PAK (68 kDa).

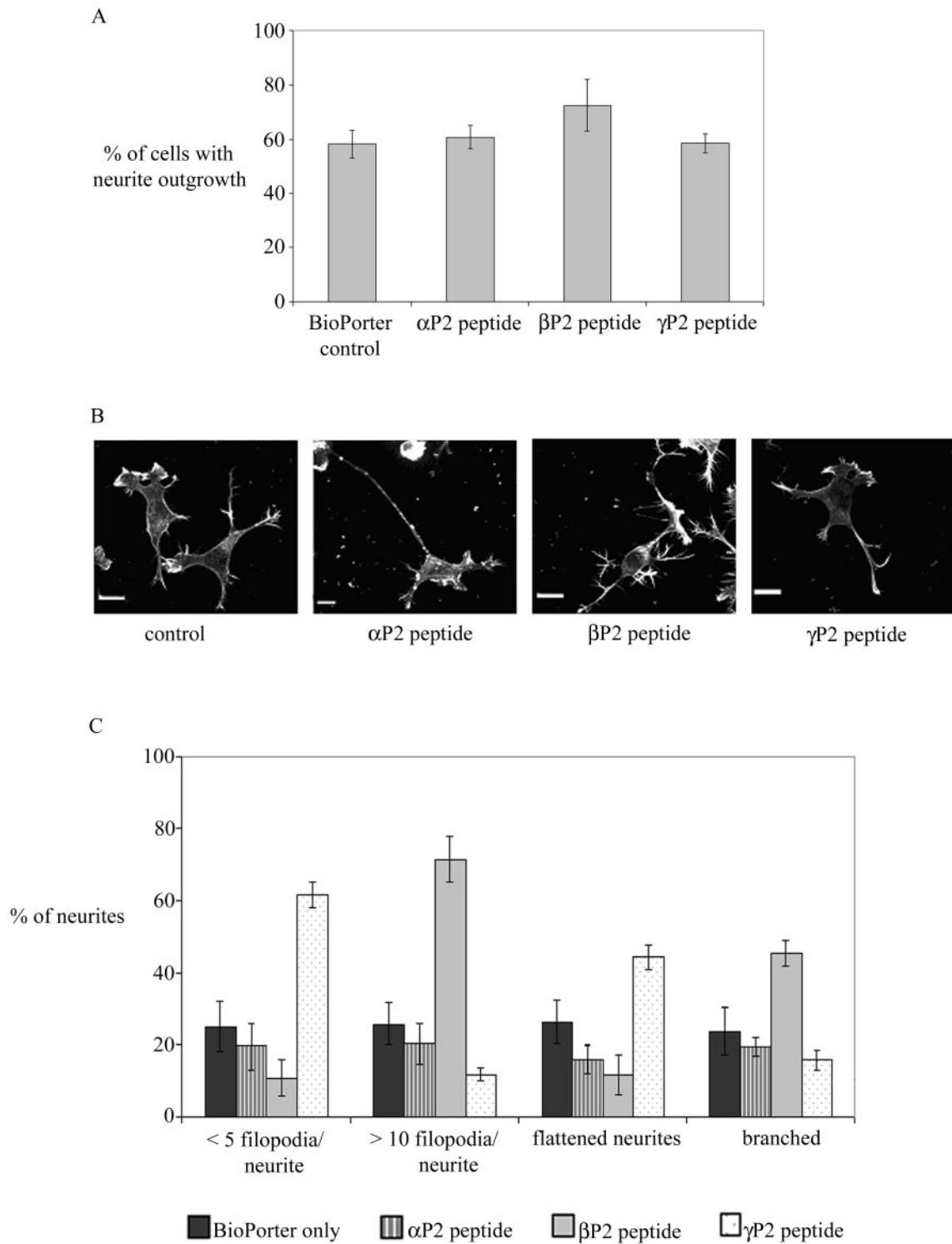
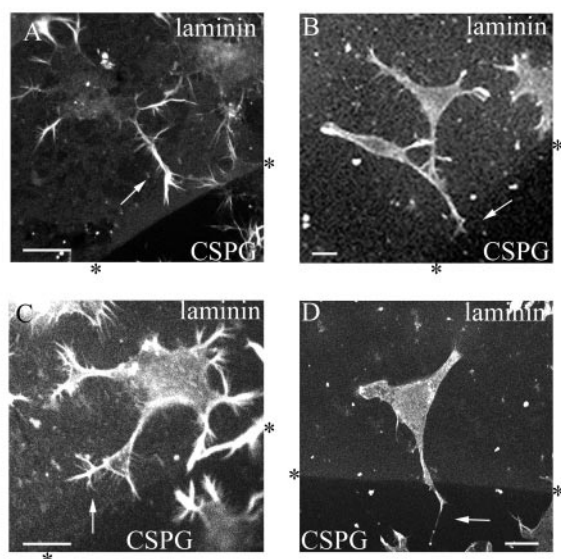


FIG. 8. Effects of N-terminal PAK peptides on neurite outgrowth and morphology in serum-starved cells. (A)  $\alpha$ P2,  $\beta$ P2, and  $\gamma$ P2 peptides were delivered by BioPorter with marker IgG into serum-starved cells. Control cells received BioPorter-delivered IgG marker only. IgG-containing cells were stained with phalloidin. The results are for three independent experiments ( $n = 6$  for the control and peptide-containing cells). (B) Morphology of neurites of serum-starved cells containing PAK peptides. The results are for three independent experiments ( $n = 6$  for all conditions). The categories of neurite morphology are as defined in the legend to Fig. 3.



E

Laminin/CSPG	Stop	Turn	Cross
Control	28.27 ± 3.94	55.51 ± 5.77	16.22 ± 4.59
αP2	41.63 ± 4.49	44.18 ± 4.41	14.18 ± 2.02
βP2	32.00 ± 2.46	39.18 ± 6.02	28.80 ± 6.25
γP2	17.24 ± 3.49	15.46 ± 1.69	67.30 ± 4.62

FIG. 9. Effect of N-terminal PAK peptides on the ability of neurites to guide at a laminin/CSPG boundary. Examples are given of (A) control cell-neurite stopped at boundary (arrow), (B)  $\alpha$ P2 peptide-containing cell-neurite stopped at boundary (arrow), (C)  $\beta$ P2 peptide-containing cell, neurite turning (arrow), and (D)  $\gamma$ P2 peptide-containing cell, neurite crossing (arrow). The PAK peptides were delivered by BioPorter with marker IgG to serum-starved cells. Control cells received BioPorter-delivered IgG marker only. IgG-containing cells were stained with phalloidin. Laminin/CSPG boundary was detected as in Fig. 1. (E) Analysis of guidance behavior of neurites of serum-starved cells containing PAK peptides. Neurites are categorized as showing Stop, Turn, or Cross behavior. Results are for three independent experiments ( $n = 9$  for control,  $n = 7$  for cells containing  $\alpha$ P2 or  $\beta$ P2 peptides, and  $n = 6$  for cells containing  $\gamma$ P2 peptide).

Y-27532, respectively) showed similar numbers of neurites within either the stop or turn category (Fig. 11A, B, and C). In cells containing RhoA N19, the neurites crossing appeared to be derived from those within both the stop and turn categories. As with cells containing the  $\gamma$ P2 peptide, in cells containing  $\alpha$ PAK-CAAX or  $\alpha$ PAK-CAAX KD the increased numbers of neurites crossing appeared to be mainly derived from those normally within the turn category (Fig. 11H and G). Thus, the PAK derivatives may act principally to disrupt the turning response of neurites, allowing them to cross onto the repulsive substrate.

## DISCUSSION

As with the soluble factor ACh, N1E-115 cells will respond to substrates in a directed manner. The permissive substrate laminin stimulates the Rac1 signaling pathways of N1E-115 cells through integrin receptors (20, 47, 40), with neurite outgrowth being blocked by antibody to  $\beta$ 1 integrin (40). When

grown on laminin, N1E-115 cells showed a marked avoidance of the repulsive substrates CSPG and tenascin. At the laminin/CSPG or laminin/tenascin boundary, neurites were observed to stop or turn on time-lapse analysis. The majority avoided the boundary through turning. This type of behavior is similar to that reported for chick and rat DRG when contact with either CSPG or tenascin did not promote collapse but initiated a turning behavior where filopodia were seen to extend onto the CSPG while the growth cone turned. The latter responses were also inferred from fixed and stained cells (43, 51). CSPGs present in glial scars are thought to cause a biochemical barrier to nerve regeneration (29). The CSPGs brevicain and versican purified from bovine CNS myelin preparations have been shown to inhibit neurite outgrowth from neonatal cerebral granule cells and DRG neurons (34). Tenascin is also associated with glial scarring (22, 24, 28) and contains domains that are capable of repelling cerebellar granule neurons (30).

The effects of C3 toxin indicate that inhibition of Rho pathways will promote outgrowth of neurites that are also capable of avoiding repulsive substrates. C3 toxin acts by ribosylating RhoA at asparagine-41 and the equivalent residue of the other Rho proteins, preventing the activation of RhoA, -B, and -C (32). While RhoA N19 will promote outgrowth of neurites, many of these neurites do not display the avoidance response. RhoA N19 exists as the constitutively GDP-bound form which binds to a guanine nucleotide exchange factor (GEF) but is unable to exchange the GDP for GTP, effectively preventing endogenous RhoA from being activated. Since the effect of C3 indicates that RhoA inhibition did not disrupt guidance, this suggests that RhoA N19 not only prevents activation of RhoA (leading to neurite outgrowth) but possibly that of other GTPase(s) involved in the guidance response. Indeed we have found RhoA N19 to interfere with Rac activation in N1E-115 cells (Fig. 5). Some GEFs can activate different members of the Rho GTPase family; e.g., Trio has two GEF domains, one able to activate RhoA and the other Rac1 (3). It is possible that RhoA N19 may bind such GEFs as Trio, not only preventing activation of RhoA but also perhaps that of Rac1, which is normally required for the guidance response. Both Trio and Rac1 participate in guidance of photoreceptor axons in *Drosophila* eyes. Mutations involving Trio, Rac1, or PAK disrupt the normal pathfinding of these cells towards the lamina and medulla. For correct guidance of photoreceptor axons, Trio is required to activate Rac1, and in response to a separate signal, PAK is recruited to membrane receptors by binding to the Nck homologue DOCK and is then activated by Rac1 (33).

Sung et al. (44) have also suggested that another pathway apart from that involving RhoA and ROK might be concerned with regeneration since both Y-27632 and C3 toxin were ineffective in promoting recovery after spinal cord injury in rats. C3 toxin was found to be toxic, and Y-27632 delayed the recovery of injured rats. The application of fasudil (HA 1077), a less specific protein kinase inhibitor, significantly increased recovery. On the other hand, Fouriner et al., (11) reported that the application of Y-27632 increased recovery in rats that had had corticospinal tract lesions. However, they were unable to rule out the involvement of the kinase PRK2, which is also a target of Y-27632 but is less affected. That C3 toxin did not increase recovery was attributed to differences in delivery of C3 toxin and Y-27632.

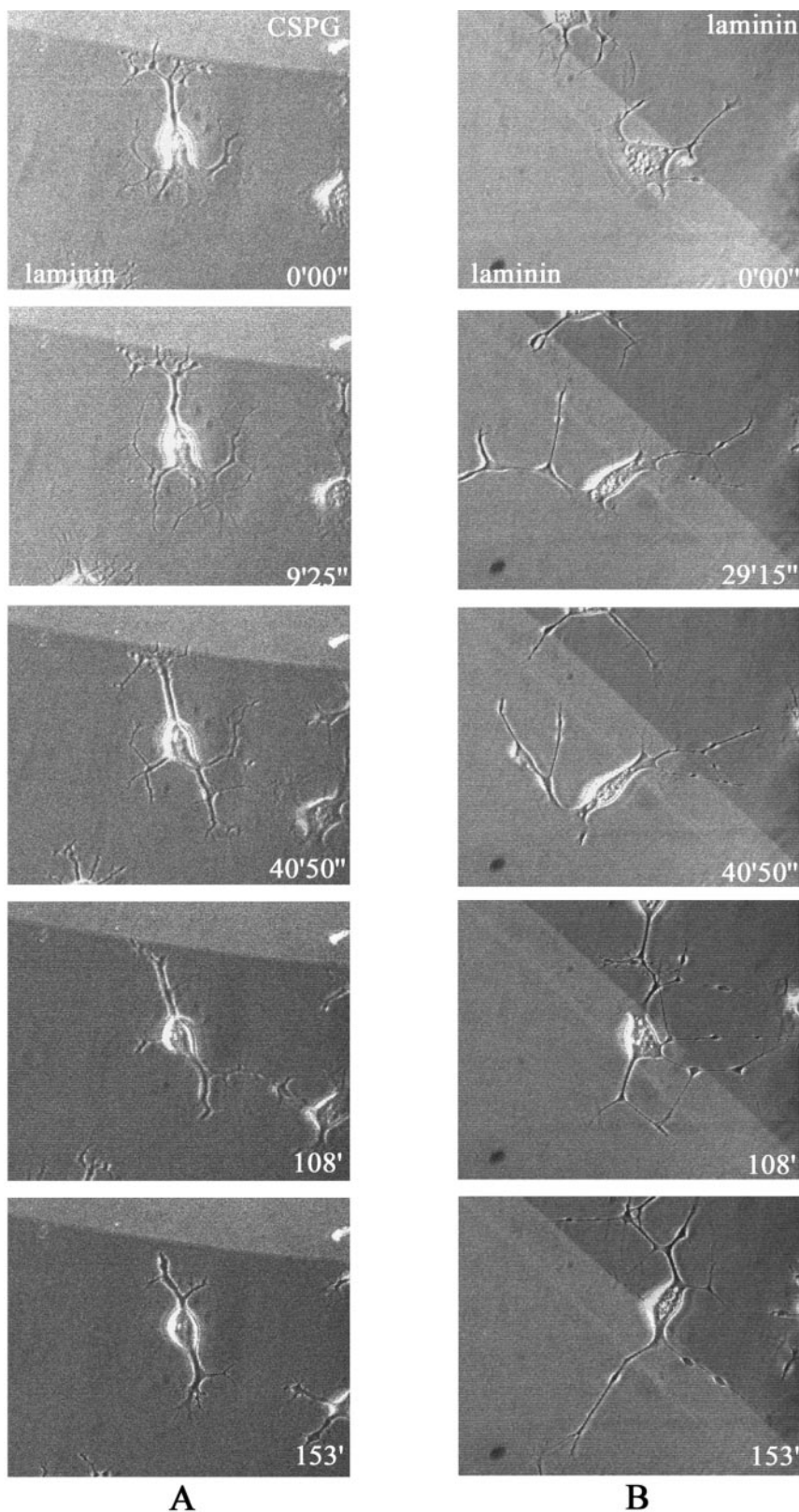


FIG. 10. Time-lapse analysis of neurites stopping at the CSPG boundary. Outgrowing cell neurites stopping and retracting at a laminin-CSPG boundary (A) or freely crossing a laminin-laminin boundary, followed by crossing of the cell body itself (B). Neurite outgrowth was induced by serum starvation and treatment with  $10 \mu\text{M}$  Y-27632. Details are given in Materials and Methods. The cells were subjected to time-lapse imaging at 45-s intervals for 2.5 h, with the first images taken 30 min after serum starvation/treatment. The phase-contrast images of cells were superimposed on fluorescent images of (A) CSPG-laminin or (B) laminin-laminin substrates, with TRITC included in the upper (A) or lower (B) substrates, using confocal microscopy.

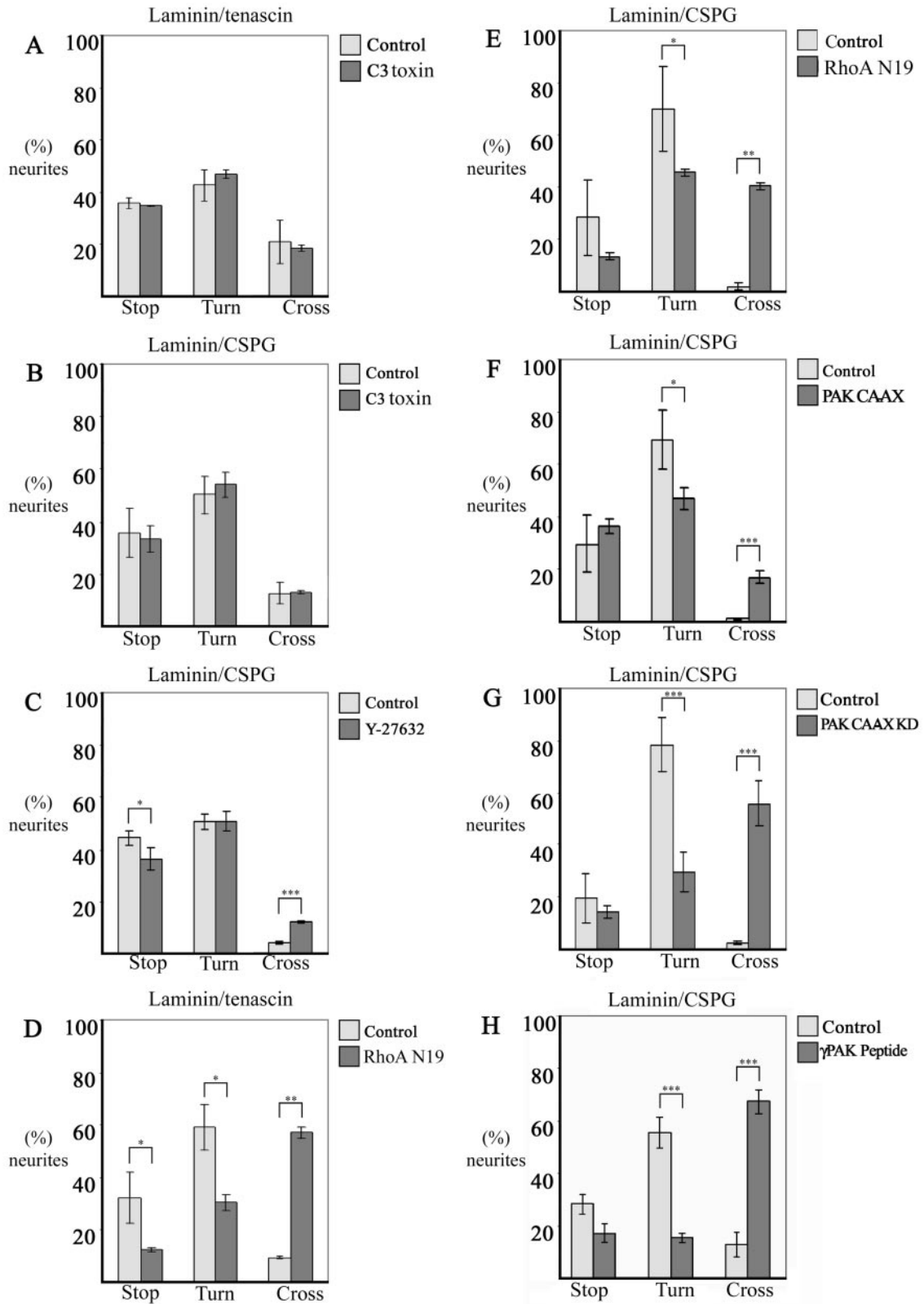


FIG. 11. Analysis of the neurite guidance behavior of cells subjected to different treatments at a laminin/tenascin (A and D) or laminin/CSPG (B, C, and E to H) boundary. Agents that have a marked effect on guidance do so mainly through disrupting the turn response. (A) C3 toxin-containing cells, (B) C3 toxin-containing cells, (C) Y-27632-treated cells, (D) RhoA N19-transfected cells, (E) RhoA N19-transfected cells, (F) PAK-CAAX-transfected cells, (G) PAK-CAAX KD-transfected cells, (H)  $\gamma$ P2 peptide-containing cells. The results were derived by subdividing neurites previously shown within the avoidance category into stop or turn categories. The cross categories are as previously determined. Error bars represent standard errors of the means. \*,  $P < 0.05$ ; \*\*,  $P < 0.01$ ; \*\*\*,  $P < 0.001$  (Mann-Whitney U test).

Concerning repulsive guidance behavior, Monnier et al. (31) reported that the inhibitory effect of CSPG on outgrowth in RGC could be blocked with Y-27632 or C3 toxin, implicating a RhoA/ROK signaling pathway. These workers used a stripe assay with alternating stripes of laminin and CSPG mixed with laminin, in which extending axons grew along the laminin stripes and avoided contact with mixed CSPG- and laminin-containing stripes. RGC previously treated with either Y-27632 or C3 toxin showed no preference between the stripes and extended their axons in a more disorganized growing pattern crossing over various stripes. The disparity between these and our findings may lie in differences in the assay and cell type used. The boundary used by Monnier et al. (31) was laminin mixed with CSPG against laminin, while we used the boundary between laminin coated over CSPG against CSPG. Further, no extrinsic factor was required for RGC outgrowth.

Studies on negative guidance signaling in mammals have implicated Rac1. Rac1 is required for the collapse of neurites evoked by Sema3A (16, 21); dominant negative Rac1 N17 but not C3 toxin blocks the collapse (16). Since Rac1 inhibition (by Rac1 N17) blocks neurite outgrowth in NIE-115 cells induced by serum starvation (20, 40), Rac1 involvement in guidance signaling could not be investigated directly in our study. Instead, the downstream Rac effector  $\alpha$ PAK was used. Because  $\alpha$ PAK does not promote the outgrowth of neurites required for the substrate boundary assay, we used the membrane-targeted  $\alpha$ PAK-CAAX, which promotes neurite outgrowth in PC12 cells (6), as well as in NIE-115 cells. The membrane-targeted form of  $\alpha$ PAK caused a significant disruption in neurite guidance at the laminin/CSPG boundary, with increased numbers crossing. Kinase-inactive  $\alpha$ PAK-CAAX KD was even more effective in this disruption. Using peptides corresponding to N-terminal amino acid residues 2 to 21 of the PAK isoforms, we found that only the  $\gamma$ P2 peptide was able to simulate the disrupting action of membrane-targeted  $\alpha$ PAK-CAAX. The  $\gamma$ P2 peptide, like the other peptides, did not affect the numbers of neurites whose outgrowth was induced by serum starvation. Time-lapse analysis of cells after delivery of the  $\gamma$ P2 peptide showed them to be deficient in producing filopodia, with some filopodium-like structures turning out to be retraction fibers that were left behind after the collapse of lamellipodia (data not shown). Moreover, the neurites were more flattened than controls and also exhibited a reduction in the number of filopodia. Given the sensory nature of filopodia, it is possible that their relative lack allows more of the filopodium-deficient neurites to extend into the hitherto repulsive substrate. Another plausible reason why the  $\gamma$ P2 peptide but not the others substantially disrupts guidance may lie in the location of  $\gamma$ - but not  $\alpha$ - or  $\beta$ PAK in filopodia.

A synthetic PAK peptide, 9-23, will prevent the second SH3 domain of Nck from binding to PAK (53). It is possible that the  $\gamma$ P2 peptide interferes with PAK activities at peripheral filopodia by sequestering Nck, whose membrane-bound DOCK homologue has been shown to participate in *Drosophila* photoreceptor axon axonal guidance (13, 33). The membrane-targeted  $\alpha$ PAK-CAAX and  $\alpha$ PAK-CAAX KD may disrupt guidance through a similar sequestration of endogenous Nck located at the membrane. Nck binding to PAK is down-regulated through PAK kinase autophosphorylation of serine (53); a prolonged binding (sequestration) of Nck may explain why

the kinase-kinase-dead PAK is a more effective disrupter. Further experiments with other PAK forms, including those incapable of binding Nck, may show how PAK operates here. Regardless of how the PAK derivatives work and which isoform is involved, our results strongly imply that PAK plays a part in the negative guidance response.

In conclusion, we show that NIE-115 neuroblastoma cells can mimic neurons in their negative guidance response and provide a facile model for studying this response. While inhibition of RhoA pathways will promote outgrowth of neurites, most of these will not cross onto unfavorable substrates. The repulsive response involves another pathway, where PAK appears to be crucially involved. To enhance regeneration and repair requiring outgrowth of neurites over normally repulsive substrates like CSPG and tenascin expressed at pathological sites/scars, mere inhibition of RhoA pathways will not be sufficient. Modulating the activities of PAK may provide yet another (additional) therapeutic avenue for partial restoration of function or combating further degeneration.

#### ACKNOWLEDGMENTS

We thank the GSK-Singapore Research Fund for their generous support.

We thank Ed Manser and Zhuo-Shen Zhao for the PAK peptides and Bhav Mehta for help with the illustrations.

#### REFERENCES

- Amano, T., E. Richelson, and M. Nirenberg. 1972. Neurotransmitter synthesis by neuroblastoma clones. *Proc. Natl. Acad. Sci. USA* **69**:258–263.
- Banzai, Y., H. Miki, H. Yamaguchi, and T. Takenawa. 2000. Essential role of neural Wiskott-Aldrich syndrome protein in neurite extension in PC12 cells and rat hippocampal primary culture cells. *J. Biol. Chem.* **275**:11987–11992.
- Bellanger, J. M., J. B. Lazaro, S. Diriong, A. Fernandez, N. Lamb, and A. Debant. 1998. The two guanine nucleotide exchange factor domains of Trio link the Rac1 and the RhoA pathways in vivo. *Oncogene* **16**:147–152.
- Benard, V., B. P. Bohl, and G. M. Bokoch. 1999. Characterization of Rac and Cdc42 activation in chemoattractant-stimulated human neutrophils using a novel assay for active GTPases. *J. Biol. Chem.* **274**:13198–13204.
- Chiquet, M., and B. Wehrle-Haller. 1994. Tenascin-C in peripheral nerve morphogenesis. *Perspect. Dev. Neurobiol.* **2**:67–74.
- Daniels, R. H., P. S. Hall, and G. M. Bokoch. 1998. Membrane targeting of p21-activated kinase 1 (PAK1) induces neurite outgrowth from PC12 cells. *EMBO J.* **17**:754–764.
- Davies, S. J., M. T. Fitch, S. P. Memberg, A. K. Hall, G. Raisman, and J. Silver. 1997. Regeneration of adult axons in white matter tracts of the central nervous system. *Nature* **390**:680–683.
- Dotti, C. G., C. A. Sullivan, and G. A. Banker. 1988. The establishment of polarity by hippocampal neurons in culture. *J. Neurosci.* **8**:1454–1468.
- Fawcett, J. W. 1992. Intrinsic neuronal determinants of regeneration. *Trends Neurosci.* **15**:5–8.
- Fawcett, J. W., and R. A. Asher. 1999. The glial scar and central nervous system repair. *Brain Res. Bull.* **49**:377–391.
- Fournier, A. E., B. T. Takizawa, and S. M. Strittmatter. 2003. Rho kinase inhibition enhances axonal regeneration in the injured CNS. *J. Neurosci.* **23**:1416–1423.
- Govind, S., R. Kozma, C. Monfries, L. Lim, and S. Ahmed. 2001. Cdc42Hs facilitates cytoskeletal reorganization and neurite outgrowth by localizing the 58-kD insulin receptor substrate to filamentous actin. *J. Cell Biol.* **152**:579–594.
- Hing, H., J. Xiao, N. Harden, L. Lim, and S. L. Zipursky. 1999. Pak functions downstream of Dock to regulate photoreceptor axon guidance in *Drosophila*. *Cell* **97**:853–863.
- Hirose, M., T. Ishizaki, N. Watanabe, M. Uehata, O. Kranenburg, W. H. Moolenaar, F. Matsumura, M. Maekawa, H. Bito, and S. Narumiya. 1998. Molecular dissection of the Rho-associated protein kinase (p160ROCK)-regulated neurite remodeling in neuroblastoma NIE-115 cells. *J. Cell Biol.* **141**:1625–1636.
- Jalink, K., E. J. van Corven, T. Hengeveld, N. Morii, S. Narumiya, and W. H. Moolenaar. 1994. Inhibition of lysophosphatidate- and thrombin-induced neurite retraction and neuronal cell rounding by ADP ribosylation of the small GTP-binding protein Rho. *J. Cell Biol.* **126**:801–810.
- Jin, Z., and S. M. Strittmatter. 1997. Rac1 mediates collapsin-1-induced growth cone collapse. *J. Neurosci.* **17**:6256–6263.

17. Jones, F. S., and P. L. Jones. 2000. The tenascin family of ECM glycoproteins: structure, function, and regulation during embryonic development and tissue remodeling. *Dev. Dyn.* **218**:235–259.
18. Katoh, H., J. Aoki, Y. Yamaguchi, Y. Kitano, A. Ichikawa, and M. Negishi. 1998. Constitutively active G $\alpha_{12}$ , G $\alpha_{13}$ , and G $\alpha_q$  induce Rho-dependent neurite retraction through different signaling pathways. *J. Biol. Chem.* **273**:28700–28707.
19. Kozma, R., S. Ahmed, A. Best, and L. Lim. 1995. The Ras-related protein Cdc42Hs and bradykinin promote formation of peripheral actin microspikes and filopodia in Swiss 3T3 fibroblasts. *Mol. Cell. Biol.* **15**:1942–1952.
20. Kozma, R., S. Sarnar, S. Ahmed, and L. Lim. 1997. Rho family GTPases and neuronal growth cone remodelling: relationship between increased complexity induced by Cdc42Hs, Rac1, and acetylcholine and collapse induced by RhoA and lysophosphatidic acid. *Mol. Cell. Biol.* **17**:1201–1211.
21. Kuhn, T. B., M. D. Brown, C. L. Wilcox, J. A. Raper, and J. R. Bamberg. 1999. Myelin and collapsin-1 induce motor neuron growth cone collapse through different pathways: inhibition of collapse by opposing mutants of Rac1. *J. Neurosci.* **19**:1965–1975.
22. Laywell, E. D., P. Friedman, K. Harrington, J. T. Robertson, and D. A. Steindler. 1996. Cell attachment to frozen sections of injured adult mouse brain: effects of tenascin antibody and lectin perturbation of wound-related extracellular matrix molecules. *J. Neurosci. Methods* **66**:99–108.
23. Letourneau, P. C., M. L. Condie, and D. M. Snow. 1994. Interactions of developing neurons with the extracellular matrix. *J. Neurosci.* **14**:915–928.
24. Lochter, A., L. Vaughan, A. Kaplony, A. Prochiantz, M. Schachner, and A. Faissner. 1991. J1/tenascin in substrate-bound and soluble form displays contrary effects on neurite outgrowth. *J. Cell Biol.* **113**:1159–1171.
25. Maekawa, M., T. Ishizaki, S. Boku, N. Watanabe, A. Fujita, A. Iwamatsu, T. Obinata, K. Ohashi, K. Mizuno, and S. Narumiya. 1999. Signaling from Rho to the actin cytoskeleton through protein kinases ROCK and LIM-kinase. *Science* **285**:895–898.
26. Manser, E., H. Y. Huang, T. H. Loo, X. Q. Chen, J. M. Dong, T. Leung, and L. Lim. 1997. Expression of constitutively active alpha-PAK reveals effects of the kinase on actin and focal complexes. *Mol. Cell. Biol.* **17**:1129–1143.
27. Margolis, R. U., and R. K. Margolis. 1997. Chondroitin sulfate proteoglycans as mediators of axon growth and pathfinding. *Cell Tissue Res.* **290**:343–348.
28. McKeon, R. J., R. C. Schreiber, J. S. Rudge, and J. Silver. 1991. Reduction of neurite outgrowth in a model of glial scarring following CNS injury is correlated with the expression of inhibitory molecules on reactive astrocytes. *J. Neurosci.* **11**:3398–3411.
29. McKeon, R. J., M. J. Jurynek, and C. R. Buck. 1999. The chondroitin sulfate proteoglycans neurocan and phosphacan are expressed by reactive astrocytes in the chronic CNS glial scar. *J. Neurosci.* **19**:10778–10788.
30. Meiners, S., M. L. Mercado, M. S. Nur-e-Kamal, and H. M. Geller. 1999. Tenascin-C contains domains that independently regulate neurite outgrowth and neurite guidance. *J. Neurosci.* **19**:8443–8453.
31. Monnier, P. P., A. Sierra, J. M. Schwab, S. Henke-Fahle, and B. K. Mueller. 2003. The Rho/ROCK pathway mediates neurite growth-inhibitory activity associated with the chondroitin sulfate proteoglycans of the CNS glial scar. *Mol. Cell. Neurosci.* **22**:319–330.
32. Nemoto, Y., T. Namba, S. Kozaki, and S. Narumiya. 1991. Clostridium botulinum C3 ADP-ribosyltransferase gene. Cloning, sequencing, and expression of a functional protein in Escherichia coli. *J. Biol. Chem.* **266**:19312–19319.
33. Newsome, T. P., S. Schmidt, G. Dietzl, K. Keleman, B. Asling, A. Debant, and B. J. Dickson. 2000. Trio combines with dock to regulate Pak activity during photoreceptor axon pathfinding in Drosophila. *Cell* **101**:283–294.
34. Niederöst, B. P., D. R. Zimmermann, M. E. Schwab, and C. E. Bandtlow. 1999. Bovine CNS myelin contains neurite growth-inhibitory activity associated with chondroitin sulfate proteoglycans. *J. Neurosci.* **19**:8979–8989.
35. Nobes, C. D., and A. Hall. 1995. Rho, rac, and cdc42 GTPases regulate the assembly of multimolecular focal complexes associated with actin stress fibers, lamellipodia, and filopodia. *Cell* **81**:53–62.
36. Postma, F. R., K. Jalink, T. Hengeveld, and W. H. Moolenaar. 1996. Sphingosine-1-phosphate rapidly induces Rho-dependent neurite retraction: action through a specific cell surface receptor. *EMBO J.* **15**:2388–2392.
37. Reier, P. J., M. J. Perlow, and L. Guth. 1983. Development of embryonic spinal cord transplants in the rat. *Brain Res.* **312**:201–219.
38. Ridley, A. J., and A. Hall. 1992. The small GTP-binding protein rho regulates the assembly of focal adhesions and actin stress fibers in response to growth factors. *Cell* **70**:389–399.
39. Ridley, A. J., H. F. Paterson, C. L. Johnston, D. Diekmann, and A. Hall. 1992. The small GTP-binding protein rac regulates growth factor-induced membrane ruffling. *Cell* **70**:401–410.
40. Sarnar, S., R. Kozma, S. Ahmed, and L. Lim. 2000. Phosphatidylinositol 3-kinase, Cdc42, and Rac1 act downstream of Ras in integrin-dependent neurite outgrowth in N1E-115 neuroblastoma cells. *Mol. Cell. Biol.* **20**:158–172.
41. Sekine, A., M. Fujiwara, and S. Narumiya. 1989. Asparagine residue in the rho gene product is the modification site for botulinum ADP-ribosyltransferase. *J. Biol. Chem.* **264**:8602–8605.
42. Silver, J., and J. H. Miller. 2004. Regeneration beyond the glial scar. *Nat. Rev. Neurosci.* **5**:146–156.
43. Snow, D. M., N. Mullins, and D. L. Hynds. 2001. Nervous system-derived chondroitin sulfate proteoglycans regulate growth cone morphology and inhibit neurite outgrowth: a light, epifluorescence, and electron microscopy study. *Microsc. Res. Tech.* **54**:273–286.
44. Sung, J. K., L. Miao, J. W. Calvert, L. Huang, H. H. Louis, and J. H. Zhang. 2003. A possible role of RhoA/Rho-kinase in experimental spinal cord injury in rat. *Brain Res.* **959**:29–38.
45. Tashiro, A., A. Minden, and R. Yuste. 2000. Regulation of dendritic spine morphology by the rho family of small GTPases: antagonistic roles of Rac and Rho. *Cereb. Cortex* **10**:927–938.
46. Tigyi, G., D. J. Fischer, A. Sebok, F. Marshall, D. L. Dyer, and R. Miledi. 1996. Lysophosphatidic acid-induced neurite retraction in PC12 cells: neurite-protective effects of cyclic AMP signaling. *J. Neurochem.* **66**:549–558.
47. van Leeuwen, F. N., H. E. Kain, R. A. van der Kammen, F. Michiels, O. W. Kranenburg, and J. G. Collard. 1997. The guanine nucleotide exchange factor Tiam1 affects neuronal morphology; opposing roles for the small GTPases Rac and Rho. *J. Cell Biol.* **139**:797–807.
48. van Leeuwen, F. N., C. Olivo, S. Grivell, B. N. Giepmans, J. G. Collard, and W. H. Moolenaar. 2003. Rac activation by lysophosphatidic acid LPA1 receptors through the guanine nucleotide exchange factor Tiam1. *J. Biol. Chem.* **278**:400–406.
49. Vastrik, I., B. J. Eickholt, F. S. Walsh, A. Ridley, and P. Doherty. 1999. Sema3A-induced growth-cone collapse is mediated by Rac1 amino acids 17–32. *Curr. Biol.* **9**:991–998.
50. Wahl, S., H. Barth, T. Ciossek, K. Aktories, and B. K. Mueller. 2000. Ephrin-A5 induces collapse of growth cones by activating Rho and Rho kinase. *J. Cell Biol.* **149**:263–270.
51. Williamson, T., P. R. Gordon-Weeks, M. Schachner, and J. Taylor. 1996. Microtubule reorganization is obligatory for growth cone turning. *Proc. Natl. Acad. Sci. USA* **93**:15221–15226.
52. Wilson, M. T., and D. M. Snow. 2000. Chondroitin sulfate proteoglycan expression pattern in hippocampal development: potential regulation of axon tract formation. *J. Comp. Neurol.* **424**:532–546.
53. Zhao, Z. S., E. Manser, and L. Lim. 2000. Interaction between Pak and Nck: a template for Nck targets and role of Pak autophosphorylation. *Mol. Cell. Biol.* **20**:3906–3917.
54. Zheng, J. Q., M. Felder, J. A. Connor, and M. M. Poo. 1994. Turning of nerve growth cones induced by neurotransmitters. *Nature* **368**:140–144.